ISSN 1846-6168 (Print), ISSN 1848-5588 (Online)
https://doi.org/10.31803/tg-20211201130315

Original scientific paper
Received: 2021-12-01, Accepted: 2022-03-29

Analysis of the Mechanical Behaviour for the External Fixation Device under the Impact of Torque

Nedim Pervan*, Adis J. Muminović, Elmedin Mešić, Enis Muratović, Muamer Delić

Abstract: In this research, an analysis of the mechanical behaviour for the Orthofix external fixation device under the impact of torque was performed. Research considers application of the Orthofix device on the tibia bone for the case of unstable fracture. 3D (Three Dimensional) model of the Orthofix device was created in the CATIA (Computer Aided Three-Dimensional Interactive Application) software, based on the real device construction. Structural analysis was used to monitor and analyse the stress magnitudes on the specific areas of the fixation device and fracture. With usage of the interfragmentary displacement data for the bone fragments, degrees of stiffness are introduced for the fracture and fixation device. Obtained results are used to specify the mechanical behaviour of the Orthofix fixation device.

Keywords: external fixation device; interfragmentary displacements; mechanical behaviour; principal stresses; stiffness analysis

1 INTRODUCTION

With ever increasing number of traffic accidents which involve motorcycle drivers, especially in recent years, external fixation devices are essential due to open fractures that may occure. External fixation device is a construction used for the purposes of the bone surgery and treatment of various types of trauma. These devices are used to fixate the bone fragments with application of pins, which are fastened into the bone fragments on the one side, while their other side is connected with the construction i.e. frame of the fixation device [1].

Design solutions for the fixation devices were developed along with the expansion of technology and medicine. For an example, simple design solutions accomplish fracture stability requirements, modular designs enables simple and fast utilization and circular devices with thin pins provide control of the small bone fragments. External fixation devices are often used with the adjustable couplings which enable dinamization in order of providing specific pressure on the bone segments [2].

Rapid evolution of computer sciences and software development has led to various softwares for 3D modeling and numerical analysis. In recent period, implementation of these softwares is inevitable for structural analysis of the fixation devices. With the 3D model and numerical analysis, a lot of data can be obtained, such as values of von Mises stress, displacement for the points of interest, as well as stress distributions and displacements of the fixation device itself [3-9].

The goal of this research is to examine the mechanical behaviour of the Orthofix external fixation system applied to the tibia bone under the impact of torque, for the case of unstable fracture.

2 DEVELOPMENT OF CAD MODEL

Orthofix fixation device represents one of the modern solutions developed for the needs of external fixation. Device is made of the austenite stainless steel (AISI 304 according to EN 10088 i.e. EN 58E) and anodized alloy of the aluminium (T6-7075 according to EN 573-3 i.e. AlZn5MgCu), coated with the layer of Polytetrafluoroethylene (PTFE). Fig. 1. shows the appearance of the Orthofix fixation device with distinguished aluminium and steel parts, in black and grey color, respectively.

Figure 1 Orthofix fixation device

Table 1 Mechanical properties of the Orthofix fixation device components

Component name	Standard denotation (AISI)	Standard denotation (EN)	Modulus of elasticity E (GPa)	Poisson's ratio υ	Denstiy ρ (kg/m^3)	Yield strength σ_v (MPa)
Truss	7075-T6	AlZn5MgCu	71.7	0.33	2810	460
Couplings	7075-T6	AlZn5MgCu	71.7	0.33	2810	460
Spherical joints	AISI 304	EN 58E	193	0.29	7900	205
Coupling fasteners	AISI 304	EN 58E	193	0.29	7900	205
Half-pins	1.4441	X$_2$CrNiMo18	196.4	0.3	8000	800

Aluminium is a non-magnetic and corrosion resistant in various environments, and it is also less expensive when compared to other metals. Black aluminium color for the device components is acquired with the anodizing surface treatment. Austenite stainless steel is attributed with great resilliance to intercrystalline corrosion, while it has reduced

yield strength, due to smaller proportion of carbon and a different structure. Mechanical properties of the Orthofix fixation device components are shown in Tab. 1 [10].

Development of the CAD model for the Orthofix device, based on properties of the physical model, is performed in the CATIA software. Device components are formed with the parametrization method, which enables connectivity between specific dimensions and reduces the time needed for corrections. Each component is created in the Part Design module, while complete fixation system is created by assembling these components in the Assembly Design module.

Apart from the Orthofix CAD model, tibia bone model is also created. Tibia is modeled as an ortotropic material with specifications according to Tab. 2 [11].

Table 2 Mechanical properties of the tibia bone

Property	Value
Longitudinal modulus of elasticity	22900 MPa
Tangential modulus of elasticity	10500 MPa
Normal modulus of elasticity	14200 MPa
Poisson's ratio for XY plane	0.29
Poisson's ratio for XZ plane	0.19
Poisson's ratio for YZ plane	0.31
Shear modulus for XY plane	6480 MPa
Shear modulus for XZ plane	6000 MPa
Shear modulus for YZ plane	3700 MPa
Material density	1850 kg/m^3

3 DEVELOPMENT OF FEM MODEL

Development of the FEM (Finite Element Method) model is performed in the CATIA software. One of the greatest advantages of the mentioned software is reflected in associativity, compared with other analysis softwares. This means that any change of CAD model parameters will be automatically updated in the FEM model.

FEM model development starts with discretization and selection of the finite element type. Discretization must be performed with the elements which are sufficiently small, so that usable results may be obtained. Also, the size of finite elements must be in accordance with computer performance capability [12, 13]. Components of the Orthofix fixation device are modeled with the linear and parabolic tetrahedron finite elements. Linear tetrahedrons are used for couplings, spherical joints and fasteners, while parabolic tetrahedrons are used for truss, tibia, and half-pins.

Once discretization is complete, connection properties for the Orthofix device are defined. Interaction between half-pins and bone models is established via fastened connection property (Fig. 2a). Fastened connection is a feature defined over the boundaries of the selected parts, where these parts are than handeled as one body. Second type of connection used to establish Orthofix system is contact connection property (Fig. 2b). With this connection property, penetration of bodies is restricted i.e. bodies can still move but only up to point where they reach strictly defined clearence.

Once virtual parts are applied, it is necessary to define torque. When analysing the basic strains, torque is the case where any cross-section of a rod is influenced with the external forces. This effect is reduced to a moment M_t, corresponding to a vector parallel to the longitudinal axis of the rod. This moment is called torque moment [14].

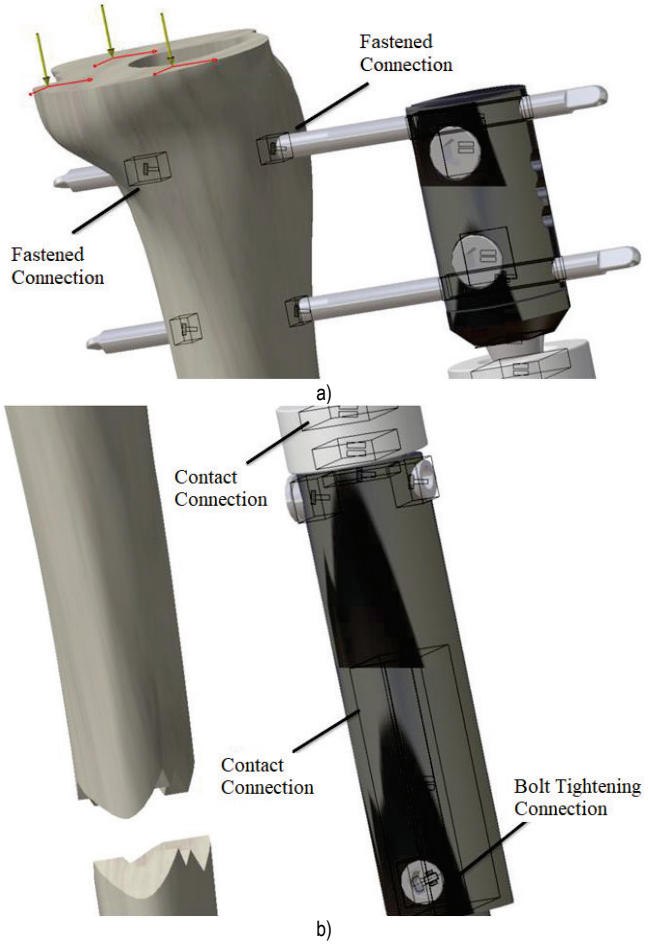

Figure 2 Connection properties for the Orthofix model: a) fastened connection, b) contact connection

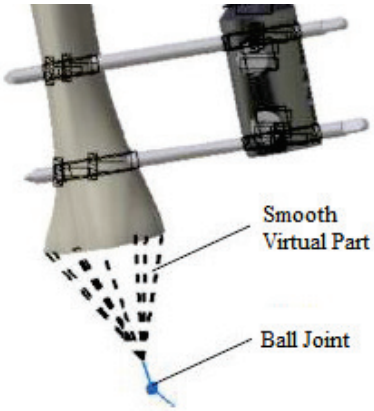

Figure 3 Fixation device model with defined virtual parts

Structural analysis of the fixation device is performed by clamping the bottom of the tibia bone model i.e. restricting all degrees of freedom. The torque moment is applied on the top of the bone model along with cylindrical joint restriction which enables one rotation about the axis of the bone model (Fig. 4).

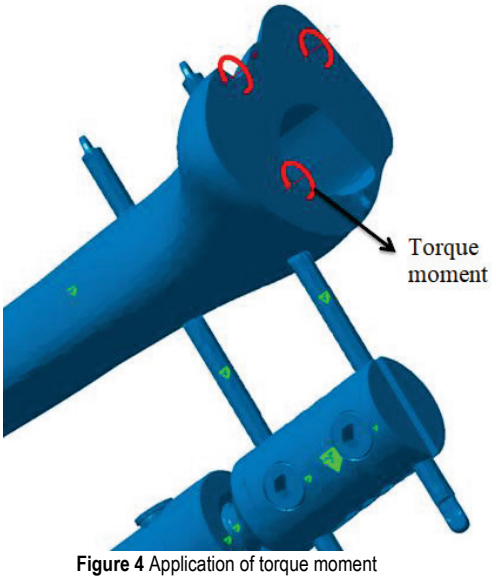

Figure 4 Application of torque moment

With the structural analysis, values of the principal stresses and von Mises stress were monitored, for the applied torque moment between the values 0 – 15 Nm. Von Mises stress is often used in the solid body mechanics and it is defined via Eq. (1) [15]:

$$\sigma_e = \sigma_{vm} = \sqrt{3J_2} = \\ = \sqrt{\frac{1}{2}\left[(\sigma_1-\sigma_2)^2+(\sigma_2-\sigma_3)^2+(\sigma_3-\sigma_1)^2\right]}. \quad (1)$$

Beside stress values, angular rotation for the appropriate bone model point was also monitored. Based on these values, Orthofix device stiffness is defined with Eq. (2) [16]:

$$C_u = \frac{M_u}{\theta}, \quad (2)$$

whereas: M_u – torque moment (Nm), θ – torque angle at the load application zone (rad).

For the purposes of stiffness definement, translational displacement for the proximal segment end point, at the load zone, is calculated (Tab. 3). These values are then translated into angular rotation via Eq. (3) [16]:

$$\tan\theta = \frac{p}{l'}, \quad (3)$$

whereas: θ – torque angle, p – translational displacement of the considered point, l – distance between axis of the segments and considered point (Fig. 5).

Without any doubt, the stiffness of the fixation device construction is important, but it does not provide direct insight about the fracture movement. More precise information may be obtained by investigating real relative movements of the bone ends under simulated load conditions.

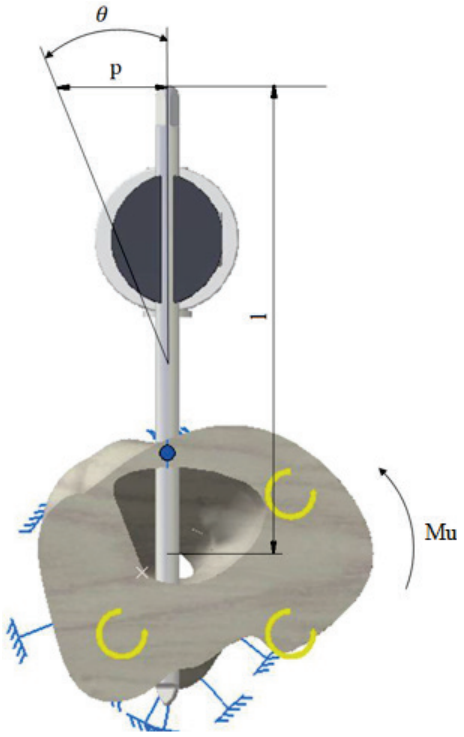

Figure 5 Displacement of the segmetns undert the impact of torque

In order to define fracture stiffness, a displacement is determined for the x, y and z directions for the pair of the adjecent points on the end planes of the proximal and distal segments at the fracture zone. For these points, resulting displacement vector (R), has the maximum value.

Relative displacements ($r_{D(x)}$, $r_{D(y)}$, $r_{D(z)}$) of the considered points in the x, y and z direction are expressed by Eq. (4) [17]:

$$\begin{aligned} r_{D(x)} &= D_{p(x)} - D_{d(x)} \\ r_{D(y)} &= D_{p(y)} - D_{d(y)}, \\ r_{D(z)} &= D_{p(z)} - D_{d(z)} \end{aligned} \quad (4)$$

Fracture stiffness is defined as ratio of the applied load and resultant relative displacement for the considered pair of points, as shown with Eq. (5) [16]:

$$C_{pu} = \frac{M_u}{R} = \frac{M_u}{\sqrt{(r_{D(x)})^2+(r_{D(y)})^2+(r_{D(z)})^2}}. \quad (5)$$

4 RESULTS

Fig. 6. shows the displacement vectors of the points under the maximum torque load. Direction, course and the intensity of the vectors are clearly noticeable. Components of the displacement vector can also be determined (Tab. 3).

In order to analyse the stiffness of the construction under the impact of torque, displacement in the y direction, of the central point at the proximal segment load zone, was observed. With usage of Eq. (4), relative displacements for

the end points of the proximal and distal segments are determined.

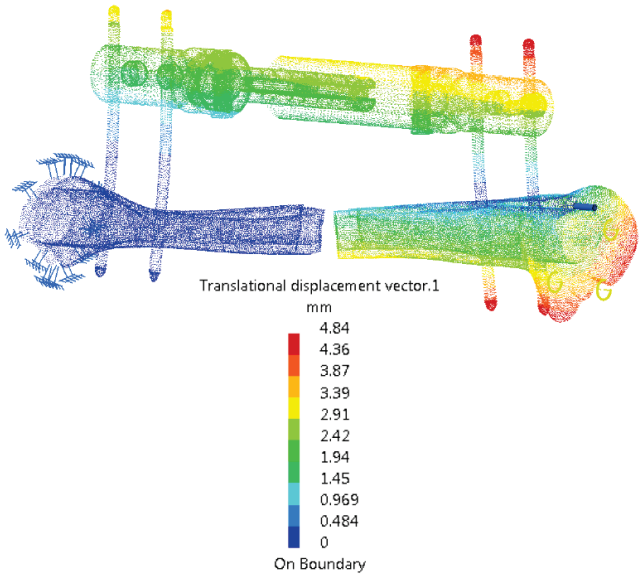

Figure 6 Displacement vectors under the impact of maximum torque

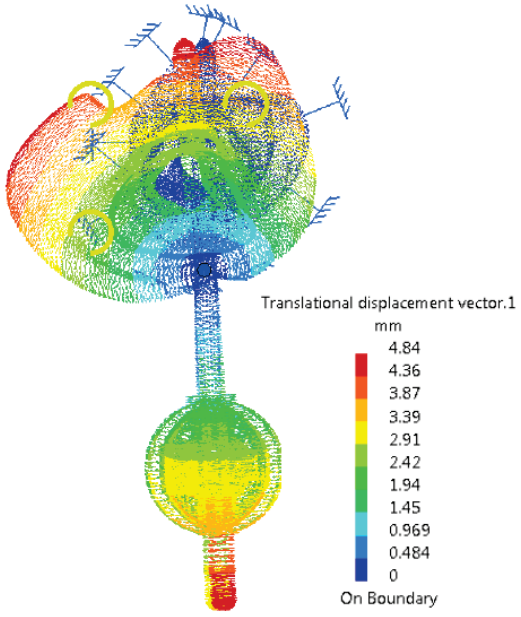

Figure 7 Displacement vectors in the load zone, under the impact of maximum torque

Angular rotation and displacement of the points for the bone model in the load zone, under the impact of the maximum torque, are shown in Fig. 7.

Values of the displacements for the maximum torque moment of 15 Nm, are presented in Tab.3.

For the maximum torque, greatest displacement of the fracture area amounts 4.84 mm and it is located at the top of the bone model i.e. brim of the upper segment. Greatest displacement for the fixation construction is located at the top and at the end of the half-pins, and it amounts 4.84 mm.

Stress values are variable and dependant of the construction shape. Most critical and most loaded zones of the construction are half-pins and contact areas between half-pins and couplings (Fig. 8).

Table 3 Displacement and stiffness values

Displacement of the proximal segment (mm)	Load zone	x	0.031
		y	1.49
		z	0
	Fracture zone	$D_{p(x)}$	0.0021
		$D_{p(y)}$	–0.26
		$D_{p(z)}$	3.24
Displacement of the distal segment (mm)	Fracture zone	$D_{d(x)}$	0
		$D_{d(y)}$	0.027
		$D_{d(z)}$	0
Torque angle (rad)		θ	0.083
Fracture stiffness (Nm/mm)		C_{pu}	3.875
Construction stiffness (Nm/rad)		C_u	180.72

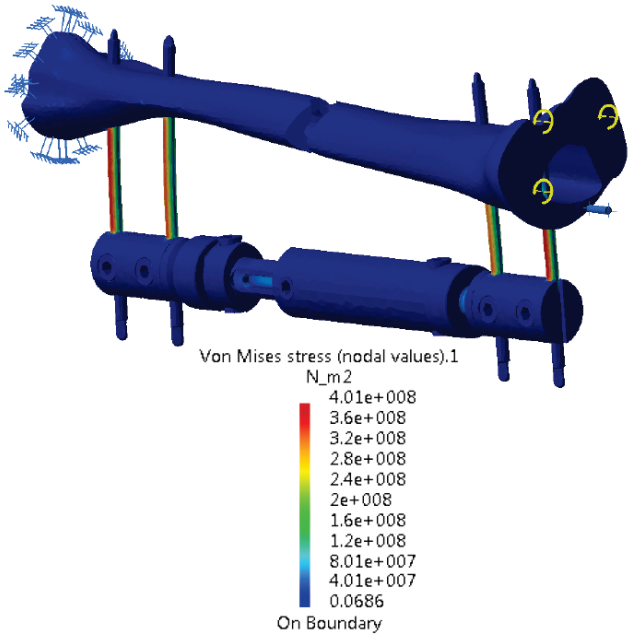

Figure 8 Distribution of the von Mises stress

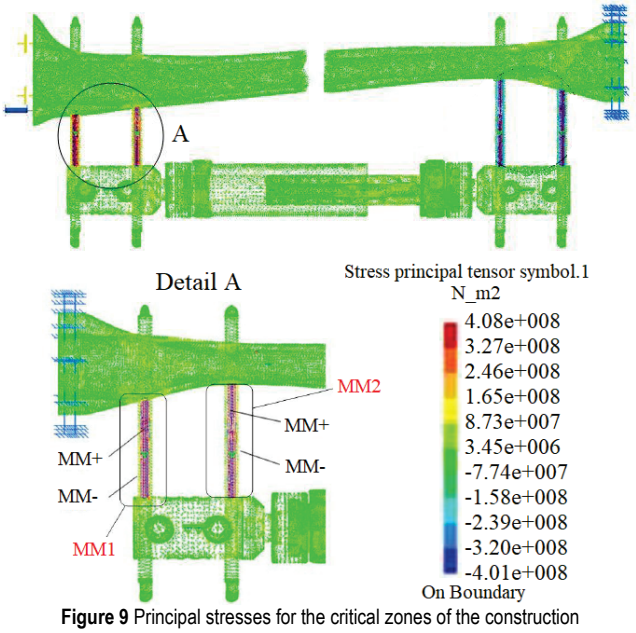

Figure 9 Principal stresses for the critical zones of the construction

These critical zones are used to collect data about intensity and direction of principal stresses (Fig. 9). Result of the 2 observed zones (MM1 & MM2) are shown in Tab. 4.

Table 4 Stress values for the maximum torque

Measuring point			MM1	MM2
Principal stresses for the fixation device critical zones (MPa)	MM+	σ_1	269.21	118
		σ_2	–4.25	4.17
		σ_3	–6.90	–11.50
	MM–	σ_1	119.36	13.30
		σ_2	–0.63	–0.45
		σ_3	–3.66	–11.80
Von Mises stress for the fixation device critical cross-section (MPa)	MM+	σ_{vm}	274.79	122.40
	MM–	σ_{vm}	121.53	21.76

5 CONCLUSION

Mechanical behaviour of the external fixation device have an enormous impact on the fracture treatment, by influencing the biomechanical fracture environment. The main task of the external fixation device is to stabilise the fracture during the treatement. In order of accomplishing this task without any mistakes and defects, it is necessary to adjust the size, shape and the relative position for each of the fixation device component. This adjustements need to correspont to the clinical needs i.e. information about the constructive parameters and loads are mandatory for the construction process.

In this research, an analysis of the mechanical behaviour for the Orthofix fixation device under the impact of torque was performed. With usage of the CATIA software, 3D model of the fixation device was formed. This model is fundamental for further FEM analysis, used for observing mechanical behaviour of the fixation device, which involve fracture movements, construction behavior under load and stiffness definition.

Structural analysis showed that maximum displacement of the fracture is located at the top of the tibia bone model with value of 4.84 mm, while maximum fixation construction displacement also amounts 4.84 mm, and it is located at the top and at the bottom of the half-pins. Displacements for the distal bone segment have small values, due to clamp restrain.

Using the displacement values for the fracture zone, obtained with analysis, fracture stiffness which amounts 3.875 Nm/mm is defined. Similarly, using the values of the angular rotation of the bone model, construction stiffness which amounts 180.72 Nm/rad is defined. Both of the defined stiffnesses satisfy the permitted limits for these types of constructions.

Values and directions of the principal stresses were observed for the 2 critical zones under the impact of maximum torque load. These zones are half-pins and area of the connection of the half-pins and couplings. Greatest stress is located on the critical zone 1 (MM1) and amounts 274.79 MPa, which satisfies the permitted stress value for the half-pin material.

By analysing the intensities and directions of the principal stresses it is noticeable that the truss is conducted to the effects of the uneven stresses of tension and pressure in two perpendicular directions, due to length of threaded connection and the bone asymmetry.

Based on the presented results and their analysis, it can be concluded that Orthofix device shows good mechanical behaviour under the impact of torque. These behaviour can be further improved by using new materials for fixation device components or with redesign process of the device.

6 REFERENCES

[1] Koo, T. K. K., Chao, E. Y. S., & Mak, A. F. T. (2005). Fixation Stiffness of Dynafix Unilateral External Fixator in Neutral and Non-neutral Configurations. *Bio-Medical Materials and Engineering*, 15, 433-444. https://pubmed.ncbi.nlm.nih.gov/16308459/

[2] Behrens, F. (1989). General Theory and Principles of External Fixation. *Clinical Orthopaedics and Related Research*, 241, 15-23. https://pubmed.ncbi.nlm.nih.gov/2647333/

[3] Behrens, F. (1989). A primer of fixator devices and configurations. *Clinical Orthopaedics and Related Research*, 241, 5-14. https://pubmed.ncbi.nlm.nih.gov/2924480/

[4] Moroz, T. K., Finlay, J. B., Rorabeck, C. H., & Bourne R. B. (1988). Stability of the Original Hoffmann and AO Tubular External Fixation Devices. *Medical & Biological Engineering & Computing*, 26, 271-276. https://doi.org/10.1007/BF02447080

[5] Oh, J. K., Lee, J. J., Jung, D. K., Kim, B. J., & Oh, C. W. (2004). Hybrid External Fixation of Distal Tibial Fractures: New Strategy to Place Pins and Wires without Penetrating The Anterior Compartment. *Archives of Orthopaedic and Trauma Surgery*, 124, 542-546. https://doi.org/10.1007/s00402-004-0724-z

[6] Paley, D., Fleming, B., Kristiansen, T., & Pope, M. (1989) A biomechanical analysis of the Ilizarov external fixator. *Clinical Orthopaedics and Related Research, 241*, 95-105. https://pubmed.ncbi.nlm.nih.gov/2924484/

[7] Radke, H., Aron, D. N., Applewhite, A., & Zhang, G. (2006). Biomechanical Analysis of Unilateral External Skeletal Fixators Combined with IM-Pin and without IM-Pin Using Finite-Element Method. *Veterinary Surgery*, 35, 15-23. https://doi.org/10.1111/j.1532-950X.2005.00106.x

[8] Mešić, E., Pervan, N., Muminović, A. J., Muminović, A., & Čolić, M. (2021). Development of Knowledge-Based Engineering System for Structural Size Optimization of External Fixation Device. *Applied Sciences, 11*(22), 10775. https://doi.org/10.3390/app112210775

[9] Pervan, N., Mešić, E., Čolić, M., & Avdić, V. (2015). Stiffness Analysis of the Sarafix External Fixator based on Stainless Steel and Composite Material. *TEM Journal, 4*(4), 366-372. Retrieved from https://www.temjournal.com/content/44/08/TemJournalNovember2015_366_372.pdf

[10] Chao, E. Y. & Hein, T. J. (1988). Mechanical performance of the standard Orthofix external fixator. *Orthopedics, 11*(7), 1057-1069. https://pubmed.ncbi.nlm.nih.gov/3405906/

[11] Dehankar, R. & Langde, A. M. (2009). Finite element approach used on the human tibia: a study on spiral fractures. *Journal og Long Term Effects of Medical Implants, 19*(4), 313-321. https://doi.org/10.1615/jlongtermeffmedimplants.v19.i4.80

[12] Mesic, E., Pervan, N., Repcic, N., & Muminovic A. (2012). Research of Influential Constructional Parameters on the Stability of the Fixator Sarafix. *Annals of DAAAM for 2012 & Proceedings of the 23rd International DAAAM Symposium*, Vienna, Austria, 561-564. Retrieved from https://www.daaam.info/Downloads/Pdfs/proceedings/proceedings_2012/132.pdf

[13] Pervan, N., Mesic, E., Colic, M., & Avdic, V. (2016). Stiffness analysis of the sarafix external fixator of composite materials. *International Journal of Engineering & Technology, 5*(1), 20-24. Retrieved from https://www.sciencepubco.com/index.php/ijet/article/view/4912

[14] Mesic, E., Avdic, V., & Pervan, N. (2015). Numerical and experimental stress analysis of an external fixation system. *Folia Medica Facultatis Medicinae Universitatis Saraeviensis, 50(1)*, 52-58. Retrieved from http://foliamedica.mf.unsa.ba/index.php/FM/article/view/43

[15] Pervan, N., Mesic, E., & Colic, M. (2017). Stress analysis of external fixator based on stainless steel and composite material. *International Journal of Mechanical Engineering & Technology, 8*(1), 189-199. Retrieved from https://www.researchgate.net/publication/320466841_Stress_analysis_of_external_fixator_based_on_stainless_steel_and_composite_material

[16] Mešić, E., Avdić, V., Pervan, N., & Repčić, N. (2015). Finite Element Analysis and Experimental Testing of Stiffness of the Sarafix External Fixator. *Procedia Engineering*, 100, 1598-1607. https://doi.org/10.1016/j.proeng.2015.01.533

[17] Mesic, E., Avdic, V., Pervan, N., & Muminovic, A. (2015). A new Proposal on Analysis of the Interfragmentary Displacements in the Fracture Gap. *TEM Journal, 4*(3), 270-275. Retrieved from https://www.temjournal.com/content/43/06/TemJournalAugust2015_270_275.pdf

Authors' contacts:

Nedim Pervan, PhD, Associate Professor
(Corresponding author)
University of Sarajevo, Faculty of Mechanical Engineering,
Vilsonovo šetalište 9, 71000 Sarajevo, Bosnia and Herzegovina
+38733729800, pervan@mef.unsa.ba

Adis J. Muminović, PhD, Associate Professor
University of Sarajevo, Faculty of Mechanical Engineering,
Vilsonovo šetalište 9, 71000 Sarajevo, Bosnia and Herzegovina
+38733729800, adis.muminovic@mef.unsa.ba

Elmedin Mešić, PhD, Full Professor
University of Sarajevo, Faculty of Mechanical Engineering,
Vilsonovo šetalište 9, 71000 Sarajevo, Bosnia and Herzegovina
+38733729800, mesic@mef.unsa.ba

Enis Muratović, PhD Student, Teaching Assistant
University of Sarajevo, Faculty of Mechanical Engineering,
Vilsonovo šetalište 9, 71000 Sarajevo, Bosnia and Herzegovina
+38733729800, muratovic@mef.unsa.ba

Muamer Delić, PhD, Assistant Professor
University of Sarajevo, Faculty of Mechanical Engineering,
Vilsonovo šetalište 9, 71000 Sarajevo, Bosnia and Herzegovina
+38733729800, delic@mef.unsa.ba